Elucidating shared genetic association between female body mass index and preeclampsia

Check for updates

Fengmei Yang[1,6], Zhijian Zha[2,6], Fang Gao[3,6], Man Wang[1], Enfu Du[1], Ziyang Wang[4], Lei Zhou[1], Bo Gao[1], Si Li[5] & Danfeng Zhang [1] ✉

The prevalence of obesity is steadily rising and poses a significant challenge to women's health. Preeclampsia (PE), a leading cause of maternal and fetal mortality, is significantly linked to a high body mass index (BMI). However, the shared genetic architecture underlying these conditions remains poorly understood. In this study, we used summary-level data from large-scale genome-wide association studies of BMI (N = 434,794) and PE (Ncases = 8185; Ncontrols = 234,147) to assess the shared genetic architecture between them. Our findings revealed a significant genetic correlation between BMI and PE, with an estimated sample overlap of approximately 0.8%. We identified roughly 1100 shared genetic variants, with the most notable region of local genetic correlation located in 16q12.2. Enrichment analyses highlighted endothelial dysfunction as a key biological mechanism linking BMI and PE. Additionally, RABEP2 was identified as a novel shared risk gene. Mendelian randomization analysis demonstrated a bidirectional causal relationship between BMI and PE, with blood pressure identified as a key mediator. We identified the shared genetic foundation between BMI and PE, providing valuable insights into the comorbidity of these conditions and offering a new framework for future research into comorbidity.

With the improvement of socioeconomic conditions, obesity has become increasingly prevalent and has emerged as one of the major health threats[1]. Although obesity affects individuals across all age groups and genders, the prevalence of obesity is generally higher in women compared to men[2]. Additionally, certain issues, such as chronic diseases, fertility, and pregnancy outcomes, are particularly significant for women[3]. Therefore, the impact of obesity on women's health warrants further attention.

In recent years, growing evidence has indicated that obesity, defined as a body mass index (BMI) > 30, has been identified as a risk factor for preeclampsia (PE)[4,5]. PE is an inflammatory disease that occurs during pregnancy, affecting 2–8% of pregnant women, and is a leading cause of short-term morbidity and mortality for both mothers and neonates[6]. The pathogenesis of PE is thought to involve various mechanisms, including an imbalance of vascular endothelial growth factor A (VEGFA) and soluble fms-like tyrosine kinase-1 (sFlt1), placental oxidative stress, and systemic immune activation; however, the specific mechanisms remain unclear[7].

Meta-analyses and cohort studies have demonstrated that a high BMI is a significant risk factor for PE, with obese pregnant women exhibiting a higher risk of developing PE compared to those with a normal BMI[8–10]. Additionally, several Mendelian randomization (MR) studies have suggested a potential causal relationship between BMI and PE[11,12]. While these epidemiological findings offer valuable insights into the association between BMI and PE, they fall short of addressing the underlying genetic mechanisms. Investigating whether BMI and PE share genetic risk factors is crucial for unraveling their complex interplay. Notably, hypertension is closely associated with BMI, and genetic predisposition to hypertension has been linked to an increased risk of PE in European women[13,14]. Furthermore, both PE and BMI are strongly influenced by family history, underscoring the significant genetic component in their risk profiles[15,16]. These observations suggested the presence of shared underlying complex mechanisms between BMI and PE. Thus, exploring the shared genetic architecture of BMI and PE could provide crucial insights into their mechanisms and etiology.

[1]Taihe Hospital, Hubei University of Medicine, Shiyan, China. [2]College of Traditional Chinese Medicine, Hubei University of Chinese Medicine, Wuhan, China. [3]Xiangzhou District People's Hospital, Xiangyang, China. [4]Institute of Medicine Nursing, Hubei University of Medicine, Shiyan, China. [5]Department of Epidemiology and Biostatistics, School of Public Health, Tongji Medical College, Huazhong University of Science and Technology, Wuhan, China. [6]These authors contributed equally: Fengmei Yang, Zhijian Zha, Fang Gao. ✉e-mail: zdf820708@sina.com

This study aimed to investigate the shared genetic risk components between BMI and PE by leveraging large-scale genome-wide association study (GWAS) summary statistics. Unlike previous studies that primarily focused on the epidemiological association or isolated genetic factors, our research integrated genetic correlation, causal inference, and functional annotation approaches to provide a comprehensive understanding of the shared genetic architecture between BMI and PE. Through this approach, we aimed to bridge the gap between epidemiological findings and molecular mechanisms, offering novel insights into their comorbidity and underlying biological pathways.

Methods

Study design
This study utilized summary-level GWAS data to explore the potential causal relationship and shared genetic architecture between BMI and PE, with clinical samples used for validation. Summary-level GWAS data were obtained from previous meta-analyses focused on European populations. Polygenic overlap and genetic correlation between BMI and PE were evaluated using the Bivariate Causal Mixture Model (MiXeR) and linkage disequilibrium score regression (LDSC), followed by further analysis of local genetic correlations using Local Analysis of [co]Variance (LAVA) and Heritability Estimation from Summary Statistics (ρ-HESS). Cross-trait GWAS meta-analyses, including Multi-Trait Analysis of GWAS (MTAG) and Cross-Phenotype Association (CPASSOC), combined with conjunctional false discovery rate (conjFDR), were applied to identify shared risk SNPs between BMI and PE. Tissue- and cell-type-specific genetic associations were comprehensively analyzed using LDSC-seg and sclinker with data from GTEx and scRNA-seq. SNP heritability enrichment at the disease-physiological level was assessed through gene set analysis (GSA)-MiXeR, identifying relevant gene sets. Shared risk genes were identified through transcriptome-wide association studies (TWAS). Finally, causal relationships between BMI and PE were investigated using bidirectional two-sample MR. Additionally, blood pressure was analyzed to assess their potential mediating effects.

Data acquisition
GWAS data. Summary-level data for female BMI were obtained from the Genetic Investigation of Anthropometric Traits (GIANT) consortium, derived from GWAS based on participants' weight and height measurements[17]. Summary-level GWAS data for PE were sourced from FinnGen Consortium R11 (r11.risteys.finregistry.fi). Supplementary Table S1 provides details on disease endpoint codes, diagnostic information, and case-control counts. All data were restricted to European female populations, with BMI data from women aged 40–69 years and PE data from women aged 10–50 years. The PE data were based on the GRCh38 genome build, while the BMI data were based on GRCh37. For consistency, we converted the PE data to GRCh37 before conducting the analyses. In addition, the systolic blood pressure (SBP) and diastolic blood pressure (DBP) data for women were obtained from the UK Biobank, specifically from women aged 40–69 years. The inclusion criteria are detailed in Supplementary Table S1.

Transcriptome data. We used bulk-tissue RNA-seq gene expression data from the Genotype-Tissue Expression (GTEx) project (GTEx v8), which provides publicly available gene expression data across 54 primary tissues from non-diseased individuals[18]. Additionally, we used summary-level data from the GTEx v8 expression quantitative trait loci (eQTL) analysis and from eQTLGen, a large-scale meta-analysis of eQTL data involving 14,115 individuals, to identify genetic variants associated with gene expression and assess their regulatory effects[19,20].

ScRNA-seq data. We obtained single-cell sequencing data from publicly available datasets previously published, including human whole blood (85,233 cells), adipose tissue (94,415 cells), uterus (21,198 cells), and ovary (22,029 cells)[21–23].

Data analysis
Polygenic overlap analysis. MiXeR was employed to evaluate the polygenic overlap between BMI and PE, estimating genetic variants with non-zero additive genetic effects on the traits[24]. It uses a bivariate Gaussian mixture model to quantify the additive effects of single nucleotide polymorphisms (SNPs) into four categories: (1) SNPs with no effect on either phenotype, (2) SNPs specific to one phenotype, (3) SNPs specific to the other phenotype, and (4) SNPs affecting both phenotypes. Additionally, we quantified the polygenic overlap on a 0–100% scale.

Genome-wide genetic correlation analysis. LDSC is a summary statistics-based method for assessing genetic correlation from GWAS data and is typically unaffected by sample overlap[25,26]. SNPs with a minor allele frequency (MAF) ≤ 0.01 were excluded, and cleaned GWAS summary statistics were used for the analysis. We conducted unconstrained bivariate LDSC to estimate the genetic correlation (r_g) between BMI and PE. Precomputed LD scores from the 1000 Genomes Project were used for the calculation, and significant correlations were identified at $P < 0.05$. In addition, we applied a constrained intercept model assuming no sample overlap and well-corrected population stratification effects. This could improve the precision of genetic correlation estimates by reducing variance. However, if sample overlap or residual population stratification is present, this approach could introduce bias. Therefore, the results from the constrained model were interpreted cautiously and used as supplementary evidence to support the primary analysis.

Local genetic correlation analysis. LAVA is a novel statistical tool used to estimate regional genetic correlations across the genome, which provides a more granular view of local genetic correlations[27]. Bivariate LAVA analysis was conducted only for regions where both traits showed significant univariate heritability, with thresholds determined by Benjamini–Hochberg (BH) FDR, $P_{FDR} < 0.01$ was regarded as significant. LD structures were estimated using European data from Phase 3 of the 1000 Genomes Project.

To avoid false positive of local genetic correlations, we additionally applied ρ-HESS, a heritability estimation method based on summary statistics[28]. After excluding SNP with MAF ≤ 0.01 and dividing the genome into multiple non-overlapping windows (1 Mb), we calculated SNP heritability for BMI and PE within these regions and assessed their genetic correlation, applying Bonferroni correction for multiple testing.

Shared risk locus analysis. To investigate shared risk SNPs between BMI and PE, we conducted two cross-trait meta-analysis approaches: MTAG and CPASSOC. MTAG is a generalized meta-analysis method that improves the statistical power to estimate the genotype-phenotype variance-covariance matrix, enabling the generation of trait-specific effect estimates for each SNP[29,30]. SNPs with MAF ≤ 0.01 and sample size $N < (2/3) \times$90th percentile were excluded from the analysis[31]. Additionally, to account for minor sample overlap, we used bivariate linkage disequilibrium (LD) score regression to correct potential biases.

As a sensitivity analysis, we applied CPASSOC to combine evidence of association from GWAS summary statistics across multiple traits. SNP filtering was performed using PLINK with an LD threshold of $r^2 = 0.2$. In both MTAG and CPASSOC cross-trait meta-analyses, we prioritized genome-wide significant independent SNPs ($P < 5 \times 10^{-8}$) and those located in regions with significant local genetic correlations, identifying them as important regions of interest.

Next, we employed the cond/conjFDR statistical framework to refine the identification of shared risk loci, improving detection power while controlling the FDR. These frameworks leverage genome-wide shared signals by evaluating genetic overlap between traits to identify loci associated with both BMI and PE, even those not reaching genome-wide significance in traditional GWAS.

Conditional quantile–quantile (Q-Q) plots were used to visualize the enrichment of cross-trait SNPs between BMI and PE, showing the

P distribution of all SNPs in the primary trait and stratified by the significance of association in the secondary trait ($P < 0.1$, $P < 0.01$, and $P < 0.001$). Higher significance in the secondary trait was associated with stronger enrichment effects, as indicated by greater leftward deflection from the expected line.

Heritability enrichment analysis

SNP heritability enrichment at the tissue level. Using transcriptomic datasets from GTEx V8 and S-LDSC, we calculated the heritability enrichment of SNPs associated with BMI and PE across all tissue types. The significance of heritability enrichment for each tissue was assessed by the P of the regression coefficient Z-scores. To ensure robustness, we controlled for potential confounding factors, such as tissue-specific expression levels and LD structure. Tissues that remained significant after BH correction ($P_{FDR} < 0.05$) were considered enriched for both traits.

SNP heritability enrichment at the cellular level. We employed multi-marker analysis of genomic annotation (MAGMA) and the sc-linker framework, which integrates scRNA-seq, GWAS summary statistics, and epigenomic maps, to infer potential cell types where genetic variants influence disease[32,33]. ScRNA-seq datasets were used to evaluate the genetic correlation between SNPs associated with BMI and PE and cell-type-specific expression in uterine and ovarian cells. This allowed us to assess differences in BMI and PE at the cellular level.

The mean gene expression derived from adjusted scRNA-seq datasets was combined with MAGMA results for each trait to identify significantly associated cell types. BH FDR correction ($P < 0.05$) was applied to account for multiple testing.

Functional annotation of heritability. We conducted functional annotation of BMI and PE heritability using GSA-MiXeR, a novel framework based on MiXeR. This competitive GSA method quantifies the fold enrichment of partitioned heritability attributed to each gene set[34]. Gene sets selected in MAGMA analysis for BMI and PE underwent Bonferroni correction, and fold enrichment estimates computed by GSA-MiXeR were annotated to analyze the number of relevant gene sets, average fold enrichment, and average gene count. Finally, these gene sets were mapped to associated pathways to examine functional enrichment of BMI and PE traits.

Shared risk gene analysis. TWAS was used to investigate causal relationships between gene expression levels and complex traits[35]. TWAS was implemented using FUSION software, which conducted joint analyses for regions with multiple significant associations[35]. Trait-specific TWAS analyses for BMI and PE were performed separately and jointly[36] to identify shared genes and tissue expression correlations.

Gene expression weights from tissues including the uterus, ovaries, whole blood were calculated using transcriptomic data from GTEx V8. Single-trait TWAS results were intersected to identify shared gene-tissue pairs between BMI and PE. Bonferroni correction ($P < 0.05/n$) was applied to determine statistical significance, marking associations between traits and genes.

Causal relationship between PE and BMI. Bidirectional MR is a robust approach to mitigate confounding factors and reverse causality bias[37,38]. For SNP selection related to BMI, the PLINK software (https://www.cog-genomics.org/plink/) was used to extract significant ($P \leq 5 \times 10^{-8}$) and independent (kb = 10,000, $r^2 = 0.001$) instrumental variables (IVs), using the 1000 Genomes Project as a reference panel.

Causal effects were estimated using five MR methods, with inverse variance weighting (IVW) as the primary approach, complemented by MR-Egger, Bayesian weighted MR (BWMR), weighted median (WM), and robust adjusted profile score (RAPS) analyses. The F-statistic (F = BETA^2/SE^2) was calculated to evaluate the strength of IVs, with F > 10 indicating sufficient correlation between IVs and the exposure, ensuring the MR results were not biased by weak instruments[39]. Reverse MR analysis was conducted

using SNPs significantly associated with PE and BMI ($P = 10^{-8}$, $r^2 = 0.001$, kb = 10,000).

Given the results of previous steps and the associations of hypertension with BMI and PE[14], we performed mediation MR analysis to examine the roles of blood pressure, evaluating the extent to which these intermediates mediate BMI-induced PE.

Sensitivity analyses were conducted to evaluate pleiotropy and heterogeneity. MR-PRESSO was used to detect pleiotropy ($P < 0.05$ indicating the presence of pleiotropy)[40], while Cochran's Q test was used to assess heterogeneity among IVs ($P > 0.05$ indicating no heterogeneity)[41]. If heterogeneity existed (Cochran Q test $P < 0.05$), the random-effects IVW provided a reliable result[42].

Results

Polygenic overlap and genome-wide genetic correlation analysis
The univariate MiXeR analysis revealed that the number of genetic variants influencing BMI and PE were estimated to be 9.6k (SD = 0.4k) and 1.1k (SD = 0.2k), respectively, with 1.1k (SD = 0.2k) shared genetic variants between the two traits (Fig. 1A, Supplementary Table 2). Both Akaike Information Criterion (AIC) and Bayesian Information Criterion (BIC) values in the univariate analysis were positive, indicating a good model fit (Supplementary Table 2).

LDSC analysis estimated the SNP heritability (h^2) of BMI and PE to be 0.22 and 0.02, respectively (Table 1). We then applied bivariate LDSC to estimate the genome-wide genetic correlation (r_g) between BMI and PE using an unconstrained intercept, obtaining an r_g of 0.26 ($P = 1.88 \times 10^{-37}$). Examination of sample overlap across datasets revealed a minor overlap of approximately 0.8% between BMI and PE samples. When restricting the LDSC intercept, similar results were observed, with reduced significance but remaining statistically significant.

Local genetic correlation analysis
To minimize false positives, we employed two local genetic correlation methods. First, we analyzed local genetic correlations using LAVA (Supplementary Table S3). The results identified 1 genomic region with significant local genetic correlations between BMI and PE after multiple testing correction ($P_{FDR} < 0.01$). The only significant region was located on chromosome 16 (53393883–54866095) (16q12.2) (Fig. 1B).

Next, we applied ρ-HESS to further refine the analysis and enhance the precision of multi-trait colocalization. This analysis identified a total of 12 loci with significant genetic correlations ($P < 0.05$) based on SNP heritability estimates (Fig. 1C, Supplementary Table S4). After BH correction, only the region on chromosome 16 (53382572–55903774) (16q12.2) remained significant (local genetic covariance = 9.93×10^{-4}) (Supplementary Table S4).

By integrating the LAVA and ρ-HESS results, we identified the region on chromosome 16 (53393883–54866095), located in 16q12.2, as the most significant local genetic region associated with BMI and PE.

Identification of shared risk SNPs
In the cross-trait GWAS meta-analysis, we employed MTAG and CPAS-SOC methods to systematically explore the shared genetic basis between BMI and PE. No genome-wide significant SNPs in both PE and BMI were identified ($P < 5 \times 10^{-8}$, Supplementary Table S5).

To further investigate genetic variants potentially associated with BMI or PE but not reaching genome-wide significance in BMI ($P \geq 5 \times 10^{-8}$), we utilized the condFDR/conjFDR framework. Stratified Q-Q plots revealed a consistent enrichment trend for BMI SNPs conditioned on PE association P, and vice versa (Fig. 2A). Specifically, as the nominal P for PE decreased, the curves showed a significant leftward shift, indicating a notable increase in the proportion of non-zero effect SNPs for BMI as PE association levels increased. Conversely, the significance of BMI had a smaller impact on the proportion of non-zero effect SNPs in PE, suggesting that this pleiotropy might be unidirectional or mediated by other confounding factors. This observation aligns with the results from MTAG and CPASSOC, which demonstrated consistency in BMI-associated findings.
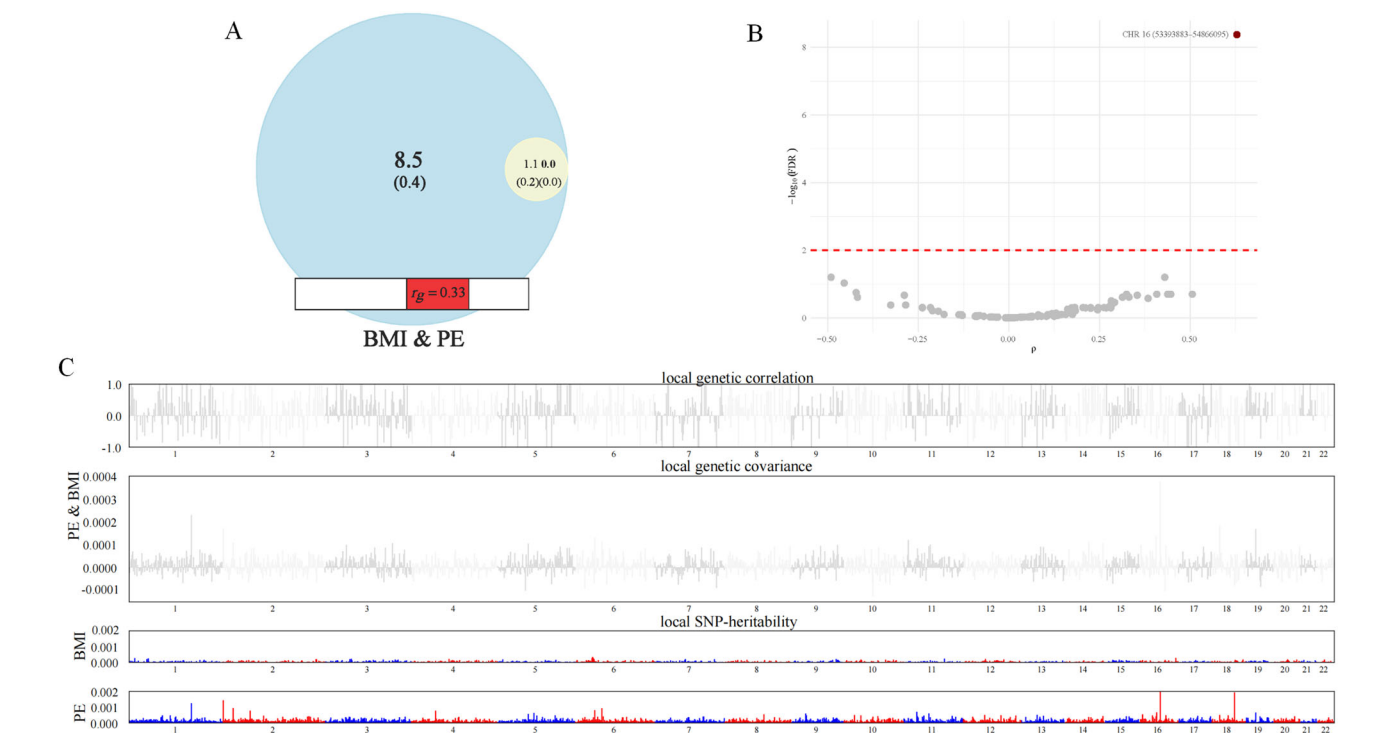
Fig. 1 | The genetic correlation between BMI and PE. A Venn diagrams of unique and shared polygenic components, showing polygenic overlap between BMI and PE. **B** LAVA analysis results depicting the genetic overlap between BMI and PE. The red dashed line indicates the significance threshold for the *P*-value. **C** The Manhattan plot of the estimates of local genetic correlation and local genetic covariance between BMI and PE, and local SNP heritability of BMI and PE, respectively. BMI body index mass, PE preeclampsia, CHR chromosome.

Under the selection threshold of $P_{conjFDR} < 0.01$, we identified 26 genomic loci shared between BMI and PE, including 12 loci with opposite directions of effect and 14 loci with the same direction of effect (Supplementary Table S6). Among these, a locus on chromosome 16 was mapped to the region identified as the most significant by LAVA analysis for BMI and PE correlation, and all were related to the FTO gene. Integrating data from BMI and PE, we ultimately identified three significant shared lead SNPs: rs2844535 on chromosome 6, rs17149871 on chromosome 8, and rs1421085 in the first intron of the FTO gene on chromosome 16 (Fig. 2B).

Additionally, we identified nine SNPs that did not reach significance in the individual analyses of BMI and PE ($P > 5 \times 10^{-8}$) but were located on chromosomes 6 and 8. Although the significance of these SNPs was limited for each trait individually, they may influence both BMI and PE through pleiotropy or complex interaction effects.

It is noteworthy that the FTO gene has long been associated with BMI, obesity and hypertension[43]. Consistent with the findings from MTAG and CPASSOC, rs1421085, located in the non-coding region of the FTO gene, is among the most obesity-associated SNPs[44].

Tissue-level SNP heritability enrichment
We evaluated tissue specificity of SNP heritability enrichment for BMI and PE. BMI showed significant enrichment in 12 tissues, primarily in the central nervous system, including the cerebellum, cerebellar hemisphere,

Table 1 | Heritability and genetic correlation between BMI and PE

	BMI	PE
h^2	0.22	0.02
r_g (No constrained intercept)	0.26 ($P = 1.88 \times 10^{-37}$)	
r_g (With constrained intercept)	0.34 ($P = 4.71 \times 10^{-19}$)	

PE preeclampsia, *BMI* body mass index, h^2 heritability, r_g genetic correlation.

substantia nigra, putamen, nucleus accumbens, hypothalamus, hippocampus, frontal cortex, cerebral cortex, caudate, anterior cingulate cortex, and amygdala (Fig. 3A, Supplementary Table S7). PE demonstrated significant enrichment in four tissues, including the ectocervix and adrenal gland (Fig. 3A, Supplementary Table S7). Notably, both BMI and PE showed significant enrichment in the cerebellum and cerebellar hemisphere.

SNP heritability enrichment at the cellular level
Through sclinker, we integrated BMI and PE GWAS data with scRNA-seq datasets from normal adipose tissue, uterus, ovary, and whole blood. We found that BMI exhibited the most significant enrichment in Myofibroblasts in adipose tissue, Glandular Cells in the uterus, Vascular Smooth Muscle in the ovary, and Alpha Beta T Cells in whole blood. For PE, the most significant enrichments were observed in Myofibroblasts in adipose tissue, Theca Stroma in the uterus, Uterine Fibroblasts in the ovary, and Memory B Cells in whole blood (Supplementary Table S8). Notably, the cells with the highest shared fold enrichment between BMI and PE were Smooth Muscle Pericytes in the uterus and Vascular Smooth Muscle in the ovary (Supplementary Table S8).

Disease-physiological SNP heritability enrichment
Using GSA-MiXeR, we identified gene sets with MAGMA *P* below 0.05 after Bonferroni correction and ranked them based on fold enrichment. Gene sets with positive AIC values in GSA-MiXeR were considered.

For BMI, we identified 96 enriched gene sets, with an average of 19 genes per set and a mean fold enrichment of 4.78 (root mean square error [RMSE]: 1.54) (Supplementary Table S9). The top 10 gene sets were primarily driven by SEC16B, FTO, BDNF, and CCNE1, and were significantly associated with pathways related to RNA and DNA demethylation, peroxisome fission, and protein localization to endoplasmic reticulum exit sites (Fig. 3B). Among the top 10 gene sets, four were driven by FTO and four by CRYZL2P-SEC16B. After excluding FTO, gene sets where FTO was the leading gene showed a significant decrease in fold enrichment, whereas sets
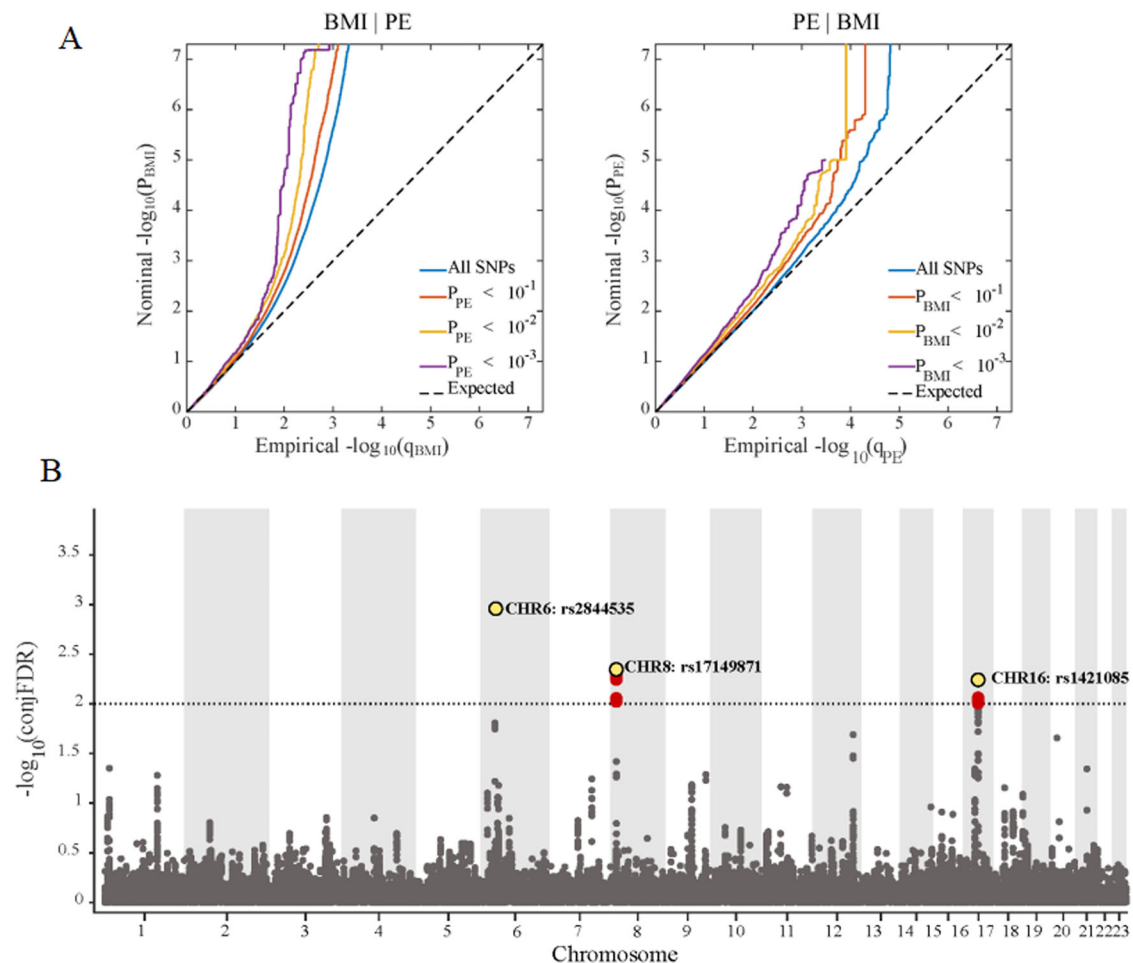
Fig. 2 | Identification of shared risk SNPs between BMI and PE. A Stratified Q-Q plots conditioned on BMI (left) and PE (right). **B** Manhattan plot of genetic associations between BMI and PE based on LAVA analysis. The *x*-axis represents chromosomal positions, and the *y*-axis shows $-\log 10(\text{conjFDR})$, indicating the statistical significance of genomic regions. The dashed line represents the significance threshold ($-\log 10(\text{FDR}) = 2$). Red points indicate significant loci with $P_{\text{FDR}} < 0.01$, and yellow points denote the leading SNPs (representative single nucleotide polymorphisms). BMI body index mass, PE preeclampsia.

driven by CRYZL2P-SEC16B exhibited minimal changes (Supplementary Table S9). This indicated substantial heterogeneity in gene enrichment within highly enriched gene sets.

For PE, we identified two enriched gene sets, with an average of five genes per set and a mean fold enrichment of 5.58 (RMSE: 2.70) (Supplementary Table S9). These sets were associated with ductus arteriosus closure and regulation of retinal ganglion cell axon guidance (Fig. 3B). The Ductus arteriosus closure gene set was primarily driven by FOXF1, while regulation of retinal ganglion cell axon guidance was driven by VEGFA (Supplementary Table S9). Notably, after excluding the leading gene, the fold enrichment for Ductus arteriosus closure decreased from 8.5 (RMSE: 3.91) to 1.5 (RMSE: 1.39), remaining above 1. In contrast, the fold enrichment for regulation of retinal ganglion cell axon guidance decreased to 0.6 (RMSE: 0.58), suggesting a critical role of VEGFA in this process.

We further estimated individual gene heritability (Supplementary Tables S10 and S11), identifying 24 shared genes with fold enrichment greater than 1 between PE and BMI. These included VEGFA and FTO, among others. Specifically, in BMI, the top two enriched genes were FTO and SEC16B, while in PE, the top two significantly enriched genes were FGF5 and ZNF831.

Shared gene identification
Through SNP heritability enrichment at the disease-physiological level, we identified shared genes between PE and BMI, including VEGFA and FTO, which have been previously reported to have significant associations with both traits[45–47]. To identify potentially novel shared genes, we utilized TWAS to integrate GWAS data for both traits with meta-analyzed eQTL data from GTEx. After stringent Bonferroni correction, we identified RABEP2 as the only gene shared between BMI and PE, enriched in blood (Supplementary Table S12).

Causal inference between BMI and PE
We conducted bidirectional MR analysis to investigate the causal relationship between BMI and PE. A total of 193 IVs were identified, all with F-statistics greater than 10 (mean = 58.40), indicating strong instrument validity. All IVs passed the directionality test (Supplementary Table S6). The MR results supported a causal effect of BMI on PE (IVW: $\beta = 0.51$ [0.44, 0.58], $P = 2.98 \times 10^{-12}$) (Fig. 4, Supplementary Table S13). It suggested that higher BMI would increase the risk of PE. Sensitivity analyses, including MR-PRESSO and Cochran's Q test, indicated no evidence of horizontal pleiotropy or heterogeneity (Supplementary Table S14).

To further investigate the role of blood pressure in the relationship between BMI and PE, we conducted a mediation MR analysis. We observed heterogeneity in the results when BMI and PE were the exposure and SBP and DBP were the outcomes (Supplementary Table S14). Therefore, we used the results from the random-effects IVW model to calculate the mediation effects of SBP and DBP. We found that SBP mediated the indirect effect of BMI on PE ($\beta = 0.08$ [0.06, 0.10]; $P = 2.2 \times 10^{-4}$), with a mediation proportion of approximately 14.71%, while DBP mediated the indirect effect of BMI on PE ($\beta = 0.13$ [0.07, 0.19]; $P = 2.4 \times 10^{-4}$), with a mediation proportion of approximately 26.35% (Supplementary Table S13).
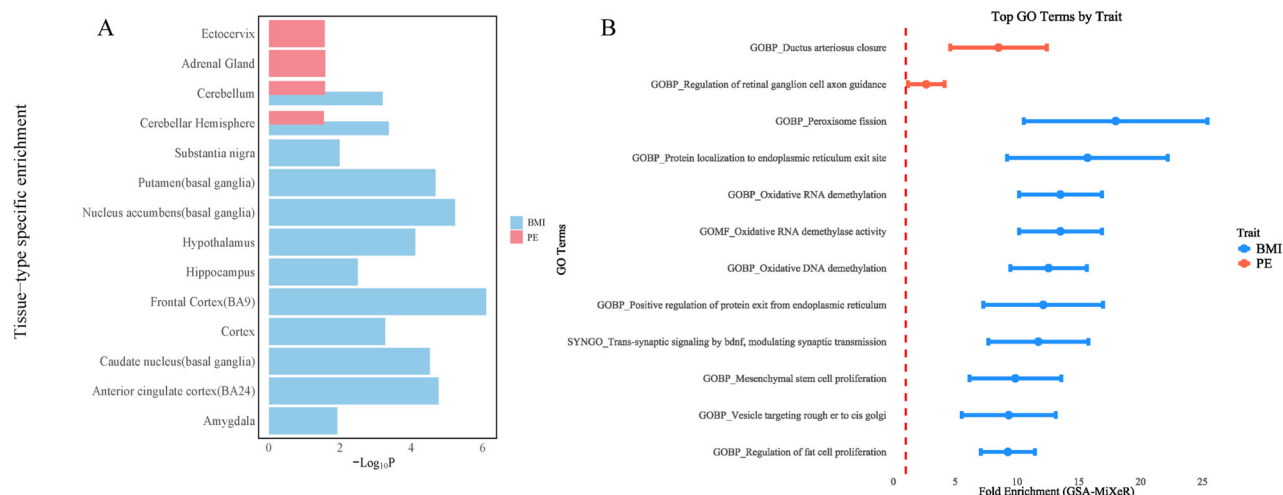
Fig. 3 | Tissue type-specific enrichment and GSA-MiXeR fold enrichment.
A Tissue type-specific enrichment of SNP heritability for BMI and PE estimated using LDSC-SEG. **B** GSA-MiXeR fold enrichment estimates for gene sets with positive AIC values. Error bars represent standard errors of the model estimates. GOMF gene ontology molecular function, GOBP gene ontology biological processes, SYNGO synaptic gene ontology, BMI body index mass, PE preeclampsia.
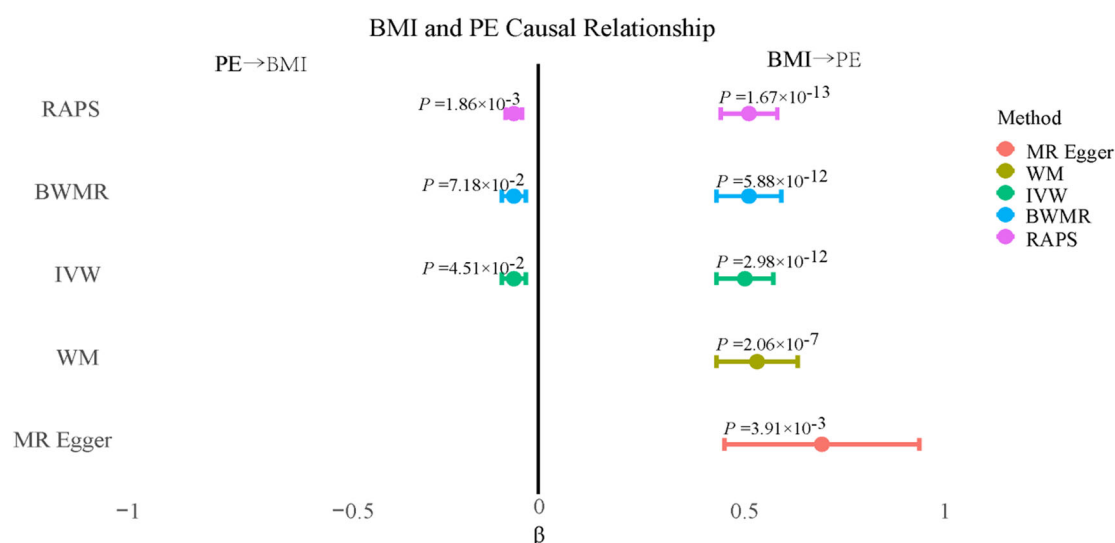

Fig. 4 | The result of MR between BMI and PE. Forest plot illustrates the bidirectional causal relationship between BMI and PE using different MR methods. *P* represents the probability of observing the results under the null hypothesis that there is no causal relationship. *P* < 0.05 indicates a potentially causal effect. The horizontal error bars represent the SE of the β. Positive β values suggest a positive causal effect, while negative β values suggest a negative causal effect. BMI body index mass, PE preeclampsia, MR Mendelian randomization, SE standard error, β regression coefficients.

In the reverse MR analysis, we screened different numbers of IVs for MR analysis in different trait pairs and found evidence supporting a potential reverse causal relationship of PE on BMI, suggesting that PE reduces the risk of developing BMI (IVW: β = −0.06 [−0.09, −0.03]; $P = 4.51 \times 10^{-2}$) (Fig. 4, Supplementary Table S13). It suggested that higher PE would decrease the risk of high BMI. Notably, when PE as exposure and BMI as outcome, we compared some large European population PE GWAS datasets used in previous studies and found that the SNPs mentioned in prior research were already included in our dataset[14,46]. Even after crossing the GWAS datasets for analysis, only 2 IVs were identified for analysis following the IV selection process described in "Methods."

In the reverse mediation analysis, although we observed that PE might increase SBP and DBP, there was no evidence of a reverse causal association between SBP, DBP, and BMI. This suggested that blood pressure might not mediate the effect of PE on the risk of developing BMI. Sensitivity analyses indicated no evidence of horizontal pleiotropy or heterogeneity (Supplementary Table S14).

Discussion

In previous studies, BMI has been established as a risk factor for PE, but no comprehensive investigation into the shared genetic architecture between BMI and PE has been conducted. We identified approximately 1.1k shared genetic variants between BMI and PE, accompanied by a strong genetic correlation. Among these, 53393883–54866095 on Chromosome 16 emerged as the most significant locus of local genetic correlation. Furthermore, through analyses of tissue, cellular, and disease-related physiological process enrichment, we uncovered potential overlaps in the pathological mechanisms between BMI and PE, which highlighted endothelial dysfunction as a central mechanism linking these conditions. RABEP2 was identified as a novel shared risk gene, which plays an important role in VEGFA signaling pathway. Moreover, our MR analysis suggested a

potential bidirectional causal effect of BMI on PE and indicated that blood pressure played an important mediating role in the effect of BMI on PE.

The results indicated a significant genetic correlation between PE and BMI. However, in the polygenic overlap analysis, all 1.1k shared genetic variants associated with PE were entirely encompassed by those of BMI. This suggested that the genetic variants associated with PE largely represented a subset of BMI-associated variants, implying that the genetic architecture of BMI likely played a predominant role in shaping the genetic characteristics of PE. Specifically, these findings underscored the fundamental role of BMI in the development of PE, suggesting that BMI might have served as a critical upstream risk factor for PE. Moreover, the complete overlap of genetic variants pointed to the existence of shared biological mechanisms between BMI and PE, which might have indirectly or directly influenced the development of PE through the genetic background of BMI. Additionally, this finding could partly have been attributed to the lower statistical power of the PE dataset compared to the BMI dataset, potentially limiting the detection of PE-specific genetic variants.

Shared risk SNPs identified include rs2844535, rs17149871, and rs1421085 as leading SNPs, along with nine SNPs that were not individually significant in either BMI or PE. Notably, three SNPs on Chromosome 8 (rs436176, rs4507762, rs4538888) are associated with the uncharacterized gene LOC105379228, which may play a role in the development of BMI and PE. Further research is needed to clarify its specific function. All identified SNPs on Chromosome 16 are associated with the FTO gene, located in the most significant locus of local genetic correlation between BMI and PE on 16q12.2[48–50]. This region highlights the potential involvement of FTO in the comorbidity of BMI and PE[48–50]. FTO is a well-known obesity-associated gene and is linked to endothelial dysfunction[51–53]. Interestingly, some SNPs in the FTO region exhibit opposing effects on BMI and PE, while others show consistent effects, suggesting a multifaceted role of FTO in the shared pathology of BMI and PE, potentially involving distinct genetic mechanisms at different loci. Shared enriched genes between BMI and PE include FTO and VEGFA. VEGFA, a key signaling protein involved in angiogenesis, vascular permeability regulation, and immune cell recruitment, is implicated in endothelial dysfunction.[60] Notably, some shared genes, such as FGF5, ZNF831, FTO, and VEGFA, have previously been identified as risk genes for hypertension and PE in earlier studies[14]. Further research is warranted to explore the roles of these genes in the link between BMI and PE.

Our findings on tissue enrichment indicated that BMI was closely associated with brain structures[54–56]. For PE, enriched tissues include the cervix, cerebellum, and adrenal glands, suggesting potential links to hormonal levels, neural regulation, and cervical status. Previous research has highlighted a connection between cerebellar abnormalities and the neurotoxicity of PE, although the specific role of cerebellar function in PE remains unclear[57]. These observations proposed a novel perspective: BMI might contribute to PE development through its effects on the cerebellum. Besides, the enrichment results of cell level revealed that smooth muscle pericytes in the uterus and vascular smooth muscle in the ovary exhibit the highest fold enrichment in both BMI and PE, suggesting that these two cell types might play crucial roles in BMI-induced PE. Notably, Smooth Muscle Pericytes in the uterus are a type of mural cell in microvasculature, involved in endothelial function regulation[58]. Endothelial dysfunction, in turn, has long been recognized as a key contributor to PE pathogenesis[59]. Similarly, Vascular Smooth Muscle in the ovary is involved in uterine spiral artery remodeling, a process implicated in the development of PE[48]. These findings suggested that BMI might induce PE by disrupting endothelial cell function in the uterus and ovary.

Notably, the results of this study highlighted that endothelial dysfunction played a critical role in the comorbidity of BMI and PE. The role of endothelial dysfunction in the development of BMI and PE as independent conditions has been extensively studied[7,49]. However, its contribution to the comorbidity of BMI and PE remains unclear. Both our enrichment analysis and prior studies point to the involvement of vascular smooth muscle in the ovary and pericytes in the uterus, suggesting their critical roles in the shared

pathology of BMI and PE. Additionally, our analysis identifies FTO, VEGFA, and the newly discovered shared gene RABEP2 as potential contributors to this comorbidity. These findings are all closely tied to endothelial dysfunction.

In addition, MR analysis revealed that blood pressure is a pivotal mediator in BMI-induced PE, but PE itself can decrease the risk of elevated BMI and increase the risk of elevated blood pressure. These results indicated the complex relationship between blood pressure, BMI and PE. Hypertension had a complex relationship with endothelial dysfunction, as it not only contributed to endothelial damage but byproducts of endothelial dysfunction, such as reactive oxygen species (ROS) and nitrogen oxides, also contributed to the development of hypertension[50,51]. Together, these findings suggest that endothelial dysfunction serves as a central nexus linking BMI, hypertension, and PE. While previous studies have shown that high BMI can lead to long-term endothelial dysfunction, resulting in late-onset hypertensive pregnancy disorders, the specific mechanisms remain unclear[52]. Furthermore, it is unknown whether increased hypertension susceptibility via endothelial dysfunction directly contributes to the elevated risk of PE. Additionally, TWAS analysis identified RABEP2 as a gene with regulatory functions in VEGFA signaling[53], but its role in BMI and PE has yet to be experimentally validated. Future research should focus on elucidating how BMI, hypertension, and PE are interconnected through endothelial dysfunction and explore the roles of genes such as RABEP2, FTO, and VEGFA in these conditions.

Strengths

Compared to previous studies, our research offers the following strengths: First, we systematically assessed the shared genetic architecture and local genetic correlations between BMI and PE, which provided a new framework for future comorbidity research. Second, we identified the mediating role of blood pressure in the relationship between BMI and PE. Lastly, we highlighted endothelial dysfunction as the core of the comorbidity between BMI and PE and identified RABEP2 as a new potential shared risk gene, providing a theoretical basis for future research.

Limitations

However, this study has several limitations. First, we found the extent of sample overlap and found that the overlap between BMI and PE GWAS datasets is approximately 0.8%. Although this overlap is relatively low, we acknowledge its potential influence on the results, so we combined multiple methods to jointly reduce the bias caused by sample overlap. Second, this study was limited to individuals of European ancestry, which might restrict the generalizability of our findings to other populations, such as African and Hispanic groups, where PE incidence was higher. The lack of genetic diversity might lead to the underestimation or omission of population-specific SNP effects. Future research should prioritize diverse datasets to address these gaps and explore potential genetic heterogeneity. Then, the lack of shared SNPs identified through MTAG and CPASSOC frameworks might reflect the overwhelming influence of BMI signals, underscoring the need for more extensive PE-specific data. Fourth, the absence of individual-level data limited our ability to perform nonlinear analyses, such as age- or BMI-specific stratifications, which could yield more nuanced insights. Finally, although we have used the most recent datasets to date, the statistical power of the PE datasets remained suboptimal, highlighting the need for larger, high-quality datasets to improve sensitivity and robustness in future analyses.

Conclusion

We identified the shared genetic architecture between BMI and PE and further pinpointed RABEP2 as a novel potential shared functional gene for these two traits. Blood pressure was found to play a crucial mediating role in the comorbidity of BMI and PE, with endothelial dysfunction emerging as the core mechanism linking BMI and PE. These findings provide new insights into the comorbidity mechanisms of BMI and PE, contributing not only to a deeper understanding of their pathogenesis but also laying a theoretical foundation for future research.

Data availability

The codes and datasets used are indicated in the "Methods" section.

Code availability

The study utilized publicly available software and tools to conduct the analyses. These include Plink (https://www.cog-genomics.org/plink/), LDSC, MiXeR (https://github.com/precimed/mixer), ρ-HESS (https://github.com/huwenboshi/hess), LAVA (https://github.com/josefin-werme/LAVA.), LDSC-seg (https://gwaslab.org/2022/03/14/ldsc-seg), MTAG, CPASSOC (https://github.com/futurologist/UKB_phenotypes_and_scripts/), ConjFDR (https://github.com/precimed/pleiofdr/blob/master/fuma/conj_fuma_combined_novelty.py), sclinker (https://github.com/karthikj89/scgenetics?tab=readme-ov-file), GSA-MiXeR (https://github.com/precimed/gsa-mixer), TwoSampleMR (https://github.com/MRCIEU/TwoSampleMR), BVMR, RAPS, and TWAS.

References

1. Caballero, B. Humans against obesity: who will win? *Adv. Nutr.* **10**, S4–s9 (2019).
2. Kanter, R. & Caballero, B. Global gender disparities in obesity: a review. *Adv. Nutr.* **3**, 491–498 (2012).
3. Tauqeer, Z., Gomez, G. & Stanford, F. C. Obesity in women: insights for the clinician. *J. Women's Health* **27**, 444–457 (2018).
4. Davenport, M. H. et al. Prenatal exercise for the prevention of gestational diabetes mellitus and hypertensive disorders of pregnancy: a systematic review and meta-analysis. *Br. J. Sports Med.* **52**, 1367–1375 (2018).
5. de Carvalho, L. S. et al. Maternal prepregnancy obesity and gestational diabetes influence on adverse perinatal outcomes. *Arch. Endocrinol. Metab.* **67**, e000605 (2023).
6. Ma'ayeh, M. & Costantine, M. M. Prevention of preeclampsia. *Semin. Fetal Neonatal Med.* **25**, 101123 (2020).
7. Phipps, E. A., Thadhani, R., Benzing, T. & Karumanchi, S. A. Pre-eclampsia: pathogenesis, novel diagnostics and therapies. *Nat. Rev. Nephrol.* **15**, 275–289 (2019).
8. Bartsch, E., Medcalf, K. E., Park, A. L. & Ray, J. G. Clinical risk factors for pre-eclampsia determined in early pregnancy: systematic review and meta-analysis of large cohort studies. *BMJ* **353**, i1753 (2016).
9. Gong, X. et al. Risk of preeclampsia by gestational weight gain in women with varied prepregnancy BMI: a retrospective cohort study. *Front. Endocrinol.* **13**, 967102 (2022).
10. Yang, Y. et al. Preeclampsia prevalence, risk factors, and pregnancy outcomes in Sweden and China. *JAMA Netw. Open* **4**, e218401 (2021).
11. Borges, M. C. et al. Integrating multiple lines of evidence to assess the effects of maternal BMI on pregnancy and perinatal outcomes. *BMC Med.* **22**, 32 (2024).
12. Venkatesh, S. S. et al. Obesity and risk of female reproductive conditions: a Mendelian randomisation study. *PLoS Med.* **19**, e1003679 (2022).
13. Landsberg, L. et al. Obesity-related hypertension: pathogenesis, cardiovascular risk, and treatment: a position paper of The Obesity Society and the American Society of Hypertension. *J. Clin. Hypertens.* **15**, 14–33 (2013).
14. Steinthorsdottir, V. et al. Genetic predisposition to hypertension is associated with preeclampsia in European and Central Asian women. *Nat. Commun.* **11**, 5976 (2020).
15. van der Sande, M. A. et al. Family history: an opportunity for early interventions and improved control of hypertension, obesity and diabetes. *Bull. World Health Organ.* **79**, 321–328 (2001).
16. Wu, C. T. et al. Association of family history with incidence and gestational hypertension outcomes of preeclampsia. *Int. J. Cardiol. Hypertens.* **9**, 100084 (2021).
17. Pulit, S. L. et al. Meta-analysis of genome-wide association studies for body fat distribution in 694 649 individuals of European ancestry. *Hum. Mol. Genet.* **28**, 166–174 (2019).
18. Battle, A., Brown, C. D., Engelhardt, B. E. & Montgomery, S. B. Genetic effects on gene expression across human tissues. *Nature* **550**, 204–213 (2017).
19. Finucane, H. K. et al. Heritability enrichment of specifically expressed genes identifies disease-relevant tissues and cell types. *Nat. Genet.* **50**, 621–629 (2018).
20. Võsa, U. et al. Large-scale cis- and trans-eQTL analyses identify thousands of genetic loci and polygenic scores that regulate blood gene expression. *Nat. Genet.* **53**, 1300–1310 (2021).
21. Jones, A. S. K. et al. Cellular atlas of the human ovary using morphologically guided spatial transcriptomics and single-cell sequencing. *Sci. Adv.* **10**, eadm7506 (2024).
22. Jones, R. C. et al. The Tabula Sapiens: a multiple-organ, single-cell transcriptomic atlas of humans. *Science* **376**, eabl4896 (2022).
23. Zhang, M. J. et al. Polygenic enrichment distinguishes disease associations of individual cells in single-cell RNA-seq data. *Nat. Genet.* **54**, 1572–1580 (2022).
24. Frei, O. et al. Bivariate causal mixture model quantifies polygenic overlap between complex traits beyond genetic correlation. *Nat. Commun.* **10**, 2417 (2019).
25. Bulik-Sullivan, B. et al. An atlas of genetic correlations across human diseases and traits. *Nat. Genet.* **47**, 1236–1241 (2015).
26. Zhang, Y. et al. Comparison of methods for estimating genetic correlation between complex traits using GWAS summary statistics. *Brief Bioinform.* **22**, bbaa442 (2021).
27. Werme, J., van der Sluis, S., Posthuma, D. & de Leeuw, C. A. An integrated framework for local genetic correlation analysis. *Nat. Genet.* **54**, 274–282 (2022).
28. Ribeiro, P. A., al Zaibag, M. & Sawyer, W. Nomenclature for the use of balloon catheters. *Am. J. Cardiol.* **63**, 262 (1989).
29. Li, X. & Zhu, X. Cross-phenotype association analysis using summary statistics from GWAS. *Methods Mol. Biol.* **1666**, 455–467 (2017).
30. Zhu, X. et al. Meta-analysis of correlated traits via summary statistics from GWASs with an application in hypertension. *Am. J. Hum. Genet.* **96**, 21–36 (2015).
31. Zeng, R. et al. Dissecting shared genetic architecture between obesity and multiple sclerosis. *EBioMedicine* **93**, 104647 (2023).
32. de Leeuw, C. A., Mooij, J. M., Heskes, T. & Posthuma, D. MAGMA: generalized gene-set analysis of GWAS data. *PLoS Comput. Biol.* **11**, e1004219 (2015).
33. Jagadeesh, K. A. et al. Identifying disease-critical cell types and cellular processes by integrating single-cell RNA-sequencing and human genetics. *Nat. Genet.* **54**, 1479–1492 (2022).
34. Frei, O. et al. Improved functional mapping of complex trait heritability with GSA-MiXeR implicates biologically specific gene sets. *Nat. Genet.* **56**, 1310–1318 (2024).
35. Zhang, Y. et al. PTWAS: investigating tissue-relevant causal molecular mechanisms of complex traits using probabilistic TWAS analysis. *Genome Biol.* **21**, 232 (2020).
36. Gusev, A. et al. Integrative approaches for large-scale transcriptome-wide association studies. *Nat. Genet.* **48**, 245–252 (2016).
37. Burgess, S., Scott, R. A., Timpson, N. J., Davey Smith, G. & Thompson, S. G. Using published data in Mendelian randomization: a blueprint for efficient identification of causal risk factors. *Eur. J. Epidemiol.* **30**, 543–552 (2015).
38. Davey Smith, G. & Hemani, G. Mendelian randomization: genetic anchors for causal inference in epidemiological studies. *Hum. Mol. Genet.* **23**, R89–R98 (2014).

39. Burgess, S. & Thompson, S. G. Avoiding bias from weak instruments in Mendelian randomization studies. *Int. J. Epidemiol.* **40**, 755–764 (2011).

40. Verbanck, M., Chen, C. Y., Neale, B. & Do, R. Detection of widespread horizontal pleiotropy in causal relationships inferred from Mendelian randomization between complex traits and diseases. *Nat. Genet.* **50**, 693–698 (2018).

41. Flatby, H. M., Ravi, A., Damås, J. K., Solligård, E. & Rogne, T. Circulating levels of micronutrients and risk of infections: a Mendelian randomization study. *BMC Med.* **21**, 84 (2023).

42. Bowden, J. et al. A framework for the investigation of pleiotropy in two-sample summary data Mendelian randomization. *Stat. Med.* **36**, 1783–1802 (2017).

43. Hernández-Caballero, M. E. & Sierra-Ramírez, J. A. Single nucleotide polymorphisms of the FTO gene and cancer risk: an overview. *Mol. Biol. Rep.* **42**, 699–704 (2015).

44. Zhang, Z. et al. The rs1421085 variant within FTO promotes brown fat thermogenesis. *Nat. Metab.* **5**, 1337–1351 (2023).

45. Dymara-Konopka, W., Laskowska, M. & Błażewicz, A. Angiogenic imbalance as a contributor of preeclampsia. *Curr. Pharm. Biotechnol.* **19**, 797–815 (2018).

46. Honigberg, M. C. et al. Polygenic prediction of preeclampsia and gestational hypertension. *Nat. Med.* **29**, 1540–1549 (2023).

47. Leong-Poi, H. Battle of the bulge: the yin and yang of vascular endothelial growth factor in obesity. *Circulation* **130**, 1034–1036 (2014).

48. Tan, B. et al. Endothelial progenitor cells control remodeling of uterine spiral arteries for the establishment of utero-placental circulation. *Dev. Cell* **59**, 1842–1859.e1812 (2024).

49. Engin, A. Endothelial dysfunction in obesity. *Adv. Exp. Med. Biol.* **960**, 345–379 (2017).

50. Montezano, A. C. & Touyz, R. M. Oxidative stress, Noxs, and hypertension: experimental evidence and clinical controversies. *Ann. Med.* **44**, S2–S16 (2012).

51. Mordi, I., Mordi, N., Delles, C. & Tzemos, N. Endothelial dysfunction in human essential hypertension. *J. Hypertens.* **34**, 1464–1472 (2016).

52. Alma, L. J. et al. Endothelial dysfunction as a long-term effect of late onset hypertensive pregnancy disorders: high BMI is key. *Eur. J. Obstet. Gynecol. Reprod. Biol.* **225**, 62–69 (2018).

53. Kofler, N. et al. The Rab-effector protein RABEP2 regulates endosomal trafficking to mediate vascular endothelial growth factor receptor-2 (VEGFR2)-dependent signaling. *J. Biol. Chem.* **293**, 4805–4817 (2018).

54. Han, J. et al. Elevated BMI impacts brain-state dynamics within the sensorimotor-to-transmodal hierarchy. *Obesity* **32**, 291–303 (2024).

55. Han, Y. P. et al. Relationship between obesity and structural brain abnormality: accumulated evidence from observational studies. *Ageing Res. Rev.* **71**, 101445 (2021).

56. Kühnel, A. et al. Stress-induced brain responses are associated with BMI in women. *Commun. Biol.* **6**, 1031 (2023).

57. Ijomone, O. K., Erukainure, O. L., Shallie, P. & Naicker, T. Neurotoxicity in pre-eclampsia involves oxidative injury, exacerbated cholinergic activity and impaired proteolytic and purinergic activities in cortex and cerebellum. *Hum. Exp. Toxicol.* **40**, 158–171 (2021).

58. Armulik, A., Genové, G. & Betsholtz, C. Pericytes: developmental, physiological, and pathological perspectives, problems, and promises. *Dev. Cell* **21**, 193–215 (2011).

59. Roberts, J. M. & Redman, C. W. Pre-eclampsia: more than pregnancy-induced hypertension. *Lancet* **341**, 1447–1451 (1993).

Author contributions

Fengmei Yang: Writing—Original Draft, Methodology. Zhijian Zha: Software, Writing—Review & Editing, Data Curation. Fang Gao: Resources, Methodology. Man Wang: Visualization, Writing—Original Draft. Enfu Du: Software. Ziyang Wang: Software, Visualization, Project administration. Lei Zhou: Methodology. Bo Gao: Methodology. Si Li: Writing—Original Draft. Danfeng Zhang: Conceptualization, Writing—Review & Editing, Methodology, Project administration, Supervision.

Competing interests

The authors declare no competing interests.

Additional information